http://ansinet.com/itj

ITJ

ISSN 1812-5638

INFORMATION TECHNOLOGY JOURNAL

ANSInet
Asian Network for Scientific Information
308 Lasani Town, Sargodha Road, Faisalabad - Pakistan

Information Technology Journal 11 (2): 225-232, 2012
ISSN 1812-5638 / DOI: 10.3923/itj.2012.225.232

Influence Analysis and Evaluation of Wheel Parameters on Motion Performance of Lunar Rover

Jicheng Liu, Senlong Tang, Pengwei Cheng and Shulin Liu
School of Mechatronic Engineering and Automation, Shanghai University, Shanghai, 200072, China

Abstract: For providing the theory basis for wheel configuration design and motion control, the rolling and steering mechanical models were developed to analyze the effect of wheel parameters on motion performance of lunar rover. And then the curves which illustrated the dependence of wheel motion performance on the wheel parameters, were deduced. The analysis results indicated that increasing the wheel diameter was more effective than increasing wheel width in enhancing the drawbar pull. In contrast, steering maneuverability was significantly affected by the wheel width. Furthermore, the dimensionless evaluation indexes were carried out to study the effect of wheel parameters on its motion performance. Five samples with different wheel width-diameter ration, namely 0.4, 0.45, 0.5, 0.55 and 0.6, were taken as the analysis object to compute the performance values such as traction performance, steering performance and overall performance index. The results revealed that the samples exhibited different superiority in single evaluation index. However, the value of comprehensive evaluation index decreases with the increasing width-diameter ratio and its maximum value appeared at about 20% slip.

Key words: Terramechanics, lunar rover wheel, performance evaluation, traction force, steering force

INTRODUCTION

Designing a lunar rover implies that the device should be constructed to accomplish many challenging tasks by traveling long distance. The successful degree of a newly designed lunar rover locomotion systems depends on how well it can operate in the rough terrains (Pandey and Ojha, 1978). Wheels play an important role in generating traction and providing locomotion for rover. However, the rover's traction performance and steering ability are dependent on the wheel parameters, namely the wheel diameter and width. When the unknown terrain is so severe that researcher can not determine which motion performance should be enhanced, it is necessary to ensure the comprehensive motion performance for lunar rover.

The traction force, produced from the interaction between the wheel and the sand, determines the rover's ability to accelerate, climb slope and cross over obstacles (Seidi *et al*., 2009). In terramechanics, the drawbar pull of a wheel is calculated by the normal and shear stresses under the wheel (Bekker, 1969; Wong, 2001). Its value can be increased by changing the wheel parameters (Liu *et al*., 2010; Ding *et al*., 2011; Ray *et al*., 2009), although it is restricted due to constraints such as vehicle dimensions and the power consumption. The previous researches (Liu *et al*., 2008, 2011) measured the traction force and steering resistance moment by changing the grouser spacing, height, thickness and circumferential angle in soil bin with loose sand. The results revealed that improvement degree of motion performance is highly dependent on the grouser height and slip. Irani *et al*. (2011) expanded on the traditional terramechanic models of Bekker and Wong to develop a new analytical model that captures the dynamic effects caused by grousers. Recently, simulation of the wheel-soil interaction was employed to investigate the wheel motion performance (Fang *et al*., 2011; Xia, 2011; Nakashima *et al*., 2011). Results indicated that the FEM and DEM model used for this study might be applicable to determine terramechanical interactions under lunar surface.

On the study of steering characteristic of vehicles, terramechanics was mainly applied to investigate the steering dynamics of mobile robot as its motion direction kept a certain angle with longitude symmetry plane of wheel (Raheman and Singh, 2003; Ishigami *et al*., 2007). Gee-Clough and Sommer (1981) adopted a dimensional analysis to study the steering forces on undriven angled wheels and revealed that the side force coefficient was related to slip angle by an exponential relationship. Furthermore, the investigation on the characteristics of wheel-sand interaction can provide the theory basis

Corresponding Author: Jicheng Liu, School of Mechatronic Engineering and Automation, Shanghai University, Shanghai, 200072, China

for the wheel robot to establish dynamic analysis (Peng *et al*., 2009; Bigdeli *et al*., 2008), path planning (Kuppan-Chetty *et al*., 2011), motion control (Yu *et al*., 2008; Zerigui *et al*., 2008) and motion evaluation (Hegazy and Dhaliwal, 2011).

The main objectives of this study are to establish the rolling and steering theoretical model for lunar rover and study the effect of wheel parameters on traction ability and steering maneuverability. Based on the analysis results, the dimensionless performance evaluation indexes and criterion for the wheel parameters is proposed in order to investigate the relationship between wheel parameters and motion performance indexes which can be beneficial to determine the wheel design parameters.

EFFECT OF WHEEL PARAMETERS ON TRACTION PERFORMANCE

Rolling mechanical model: When the driven wheel rolls on sand, the maximum radial stress occurs in front of bottom-dead-centre and shifts forward on rim, whose position is marked by angle θ_m, as shown in Fig. 1.

In Fig. 1, D and B are the wheel diameter and width, respectively. W is the payload acting on the wheel. T_r is the driving torque. P_D is the drawbar pull. θ_f, θ_r and h are the entry angle, exit angle and sinkage of the wheel, respectively. $\sigma_r(\theta)$ and $\tau_r(\theta)$ are the radial stress and shear stress acting on the intercepted cylinder.

In Fig. 1, θ_m is a function of θ_f and wheel slip, i which can be expressed as (Wong, 2001):

$$\theta_m = (c_1 + c_2 i)\,\theta_f \tag{1}$$

where, c_1 and c_2 are constant coefficients. i is the wheel slip which can be described as:

$$i = \frac{\omega D - 2v}{\omega D} \tag{2}$$

where, ω and v is the rotating angular velocity and the travel velocity of the wheel, respectively.

θ_m divides region from θ_r to θ_f into two regions, that is from θ_m to θ_f and from θ_r to θ_m. Using the Reece formulation and the relationship $h_\theta = (\cos\theta - \cos\theta_f)r$ into these two regions, the radial stress distribution $\sigma_r(\theta)$ can be described as (Wong, 2001):

$$\sigma_{r1}(\theta) = \left(k_c + k_\phi B\right)\left(\frac{D}{2B}\right)^n \left(\cos\theta - \cos\theta_f\right)^n \tag{3}$$

$$\sigma_{r2}(\theta) = \left(k_c + k_\phi B\right)\left(\frac{D}{2B}\right)^n \times \left[\cos\left(\theta_f - \frac{\theta - \theta_r}{\theta_m - \theta_r}(\theta_f - \theta_m)\right) - \cos\theta_f\right]^n \tag{4}$$

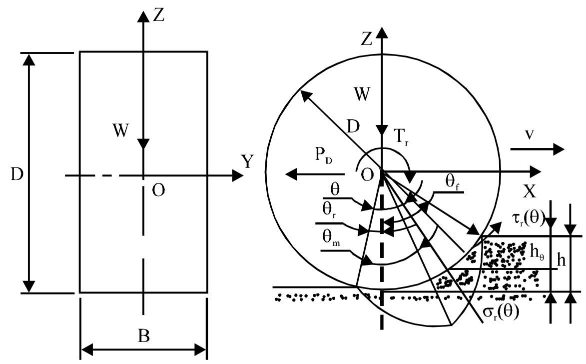

Fig. 1: Forced diagram of a driven wheel on loose sand

$$\tau_{r1}(\theta) = \left(c + \sigma_1(\theta)\tan\phi\right)\left(1 - e^{(-j/K)}\right) \tag{5}$$

$$\tau_{r2}(\theta) = \left(c + \sigma_2(\theta)\tan\phi\right)\left(1 - e^{(-j/K)}\right) \tag{6}$$

where, k_c and k_φ are the pressure sinkage modulus, n is the sinkage exponent, c is the soil cohesion, φ is the internal friction angle, K is the shear deformation modulus, j is the shear deformation distance which can be written as:

$$j = \frac{D}{2}\left[(\theta_f - \theta) - (1 - i)(\sin\theta_f - \sin\theta)\right] \tag{7}$$

Based on the force balance in the Fig. 1, the equations of W, T_r and DP can be derived by the following equations:

$$\begin{aligned} W = &\frac{DB}{2}\int_{\theta_m}^{\theta_f}\left[\sigma_1(\theta)\cos\theta + \tau_{r1}(\theta)\sin\theta\right]d\theta \\ &+ \frac{DB}{2}\int_{\theta_r}^{\theta_m}\left[\sigma_2(\theta)\cos\theta + \tau_{r2}(\theta)\sin\theta\right]d\theta \end{aligned} \tag{8}$$

$$\begin{aligned} P_D = &\frac{DB}{2}\int_{\theta_m}^{\theta_f}\left[\tau_{r1}(\theta)\cos\theta - \sigma_{r1}(\theta)\sin\theta\right]d\theta \\ &+ \frac{DB}{2}\int_{\theta_r}^{\theta_m}\left[\tau_{r2}(\theta)\cos\theta - \sigma_{r2}(\theta)\sin\theta\right]d\theta - R_B \end{aligned} \tag{9}$$

$$T_r = \left(\frac{D}{2}\right)^2 B\left(\int_{\theta_r}^{\theta_m}\tau_2(\theta)d\theta + \int_{\theta_m}^{\theta_f}\tau_1(\theta)d\theta\right) \tag{10}$$

where, R_B is the bulldozing resistance.

According to the passive earth pressure theory, bulldozing resistance acting on the area with unit width and sinkage h will be:

$$p = 0.67chK_{pc} + 0.5\gamma h^2 K_{p\gamma} \tag{11}$$

where, γ is the unit weight of sand, K_{pc}= (N_c-tanδ) $\cos^2\delta K_{pc}$, $K_{p\gamma}$ = ($2N_\gamma$/tanδ+1)$\cos^2\delta$, N_c and N_γ are the Terzaghi's bearing factors and δ = arctan (2tanφ/3).

Therefore, R_B can be expressed as:

$$R_B = B\,(0.67chK_{pc} + 0.5h^2\gamma K_{p\gamma}) \qquad (12)$$

When W, i and soil parameters are known, Eq. 1-12 describe the dependence of wheel traction performance on wheel parameters.

Theoretical effect of D and B on P_D and T_r: Defining W = 49N, i = 0.3 and the terrain parameter values described in Table 1 (Liu *et al*., 2010) in Eq. 1-12, then it can be derived the theoretical effect of D and B on P_D and T_r (as shown in Fig. 2).

It can be observed from Fig. 2a that P_D increases with the increasing D and B. However, the dependent degree of P_D on D and B is different. Increasing the wheel diameter is more effective than increasing wheel width in improving the wheel drawbar pull. This is can be explained by Eq. 9 that the larger wheel diameter is more beneficial to decrease the wheel sinkage and the bulldozing resistance will also descends with the decreasing sinkage. Meanwhile, the increasing D and B lead to the increase of driving torque as shown in Fig. 2b. The stronger traction ability is favorable to enhance the adaptability of lunar rover in strict terrain. However, the increasing driving torque implies that the driving motor will consumes much energy and this is disadvantageous for the lunar rover with limited energy. Therefore, the reasonable design of wheel parameters should comprehensively considerate the balance relation between traction performance and power consumption.

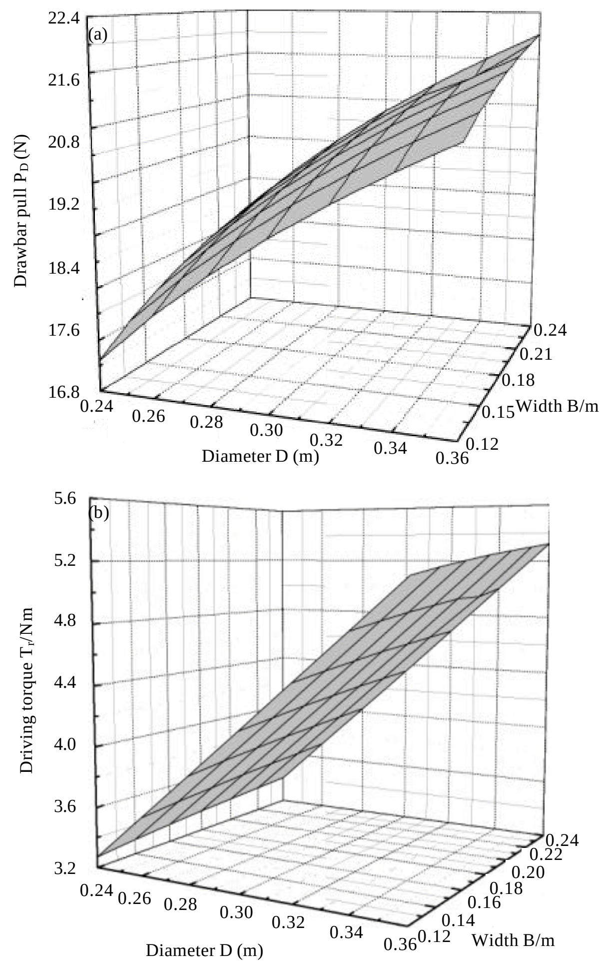

Fig. 2: Dependence of diameter and width of wheel on the P_D and T_r respectively, when W=49, I=0.3

Table 1: Mechanical parameters of sand used in the experiments

Parameter	n	k_c (N/m^{n+1})	k_φ (N/m^{n+2})	c (N/m^2)	φ (°)
Value	1.125	779.13	1.38×10^6	179.71	32.05

EFFECT OF WHEEL PARAMETERS ON STEERING MANEUVERABILITY

Steering mechanical model: Lunar rovers are expected to travel long distances to fulfill challenging mission by means of executing the remote control command. Due to the effect of unknown terrain and the time delay of information transmission between lunar rover and control center, lunar rover must steer frequently at static position in order to avoid the obstacles or change the path. For getting a rover with compact structure, researchers usually put the steering equipment above the wheel and keep the axis of steering motor passing the center of wheel. Therefore, the steering mechanical model in this paper is established for such steering motor assignation.

Figure 3 illustrates the groove and forced diagram of a steering wheel on loose sand.

In Fig. 3, the shadowed region is the horizontal projection of contact area between steering wheel and sand. T_s is the output torque of steering motor, l and ρ are the distance between the center of micro-units area dx×dy on the wheel rim and area dx×dz on the side surface of wheel and the axis O(O'), respectively.

The steering wheel will stop moving when the rover needs to change the motion direction after moving to a certain position at a slip value, i. To the closed wheel, the seven contact forces (Fig. 3). Groove and forced diagram of a steering wheel on loose sand between wheel and sand can be deduced as shown in Fig. 3. R_{SBL}, R_{SBR} and R_{SFL}, R_{SFR} are the lateral bulldozing resistance and friction force acting on both sides of wheel, respectively. R_r is the shear force acting on the wheel rim. R_{LBF} and R_{LBF} is the longitudinal bulldozing resistance acting on the wheel rim.

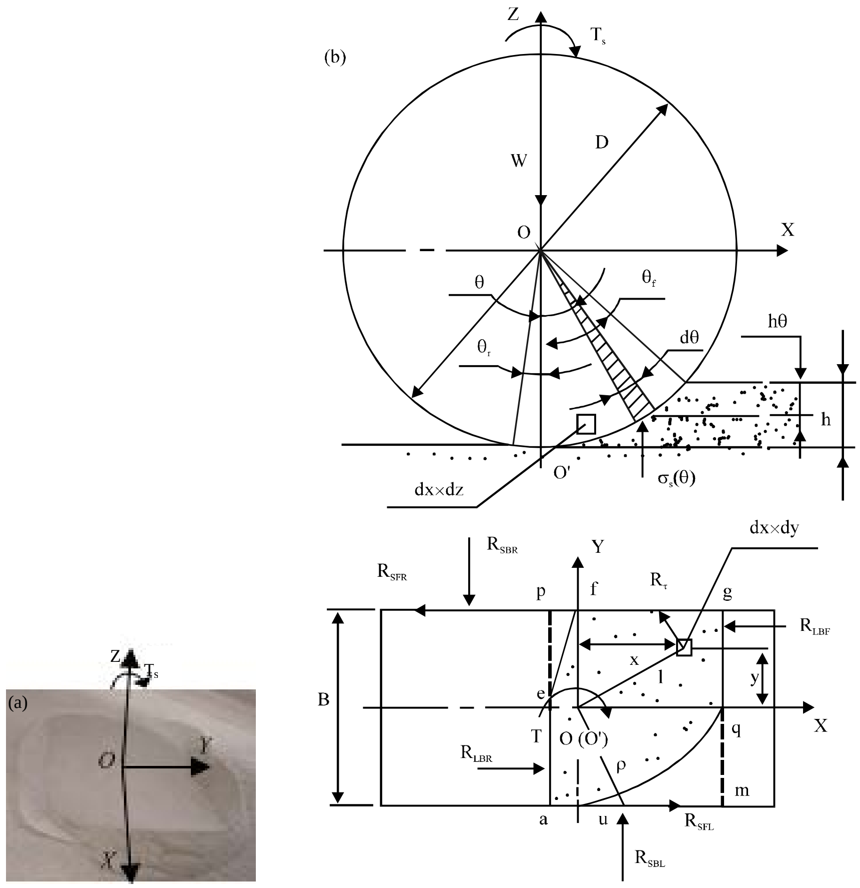

Fig. 3(a-b): (a) Groove of steering wheel and (b) Force acting on steering wheel

To calculate the moments of all of force about axis O'(O'), the resultant Steering Resistance Moment (SRM) can be derived finally.

Shear resistance moment: To take the micro-unit area dx×dy on the wheel rim as the research object as shown in Fig. 3, the distance:

$$l = \sqrt{y^2 + (0.5D\sin\theta)^2}$$

The steering wheel yaws around the axis O(O'), the shear resistance acting on the unit are dx×dy can be expressed as:

$$\tau_s(\theta) = \left(c + \sigma_s(\theta)\tan\phi\right)\left(1 - e^{(-j_s/K)}\right) \tag{13}$$

where, j_s is the shear displacement of unit area dx×dy as the wheel yaws angle β which can be given as follows:

$$j_s = l\tan\beta = \sqrt{y^2 + (0.5D\sin\theta)^2}\tan\beta \tag{14}$$

In Fig. 3, the contact area between steering wheel and sand is less than that between rolling wheel and sand. However, the sinkage is assumed to be constant, then the stress $\sigma_s(\theta)$ acting on the steering wheel rim can be defined as $\sigma_s(\theta) \approx \sigma_r(\theta)/\xi$, ξ is the ratio of contact area between steering wheel to that between rolling wheel and sand. Then, the $\sigma_s(\theta)$ can be described as:

$$\sigma_s(\theta) = \frac{1}{\xi}\left(k_c + k_\phi B\right)\left(\frac{R}{B}\right)^n \left(\cos(\theta) - \cos(\theta_f)\right)^n \tag{15}$$

Substituting Eq. 15 and 14 into Eq. 13, shear resistance acting on the rim can be derived as follows:

$$R_\tau = \xi\int_{-B/2}^{B/2}\int_{\theta_r}^{\theta_f} \tau_s(\theta) R\,dy\,d\theta$$

Thus, the shear resistance moment produced by R_τ can be written as:

$$M_\tau = \xi\int_{-B/2}^{B/2}\int_{\theta_r}^{\theta_f} \tau_s(\theta) l R\,dy\,d\theta \tag{16}$$

In Eq. 13, the value of dry sand cohesion c is smaller so that it almost can be ignored, then $\tau_s(\theta)$ is approximately proportional to $\sigma_s(\theta)$. Therefore, it can be deduced from Eq. 16 that M_τ is independent of ξ.

Longitudinal resistance moment: According to the passive earth pressure theory, bulldozing resistance acting on the rim area with unit width and h singkage will be:

$$p_{long} = 0.67chK_{pc} + 0.5\gamma h^2 K_{p\gamma} \tag{17}$$

Therefore, the R_{LBF} and R_{LBR} can be expressed as:

$$R_{LBF} = \int_0^{B/2} (0.67chK_{pc} + 0.5\gamma h^2 K_{p\gamma})dy$$

$$R_{LBR} = \int_0^{B/2} (0.67ch_r K_{pc} + 0.5\gamma h_r^2 K_{p\gamma})dy$$

where, h_r, $h_r = R(1\text{-}\cos\theta_r)$, is the sinkage of rim at the angle θ_r.

Thus, the longitudinal bulldozing resistance moment acting on the wheel rim can be written as follows:

$$\begin{aligned} M_{long} = \int_0^{B/2} & y[(0.67chK_{pc} + 0.5\gamma h^2 K_{p\gamma}) \\ & + (0.67ch_r K_{pc} + 0.5\gamma h_r^2 K_{p\gamma})]dy \end{aligned} \tag{18}$$

Lateral resistance moment: When the wheel begins to steer, the far-rear side and the near-front side of wheel from the axis O(O') will impact the sand outside and inside, respectively. The impact forces include the lateral bulldozing resistance and friction as shown in Fig. 3.

Here, taking the micro-unit area dx×dz on the contact area between wheel side and sand as the research object, the distance, ρ, can be described as:

$$\rho = \sqrt{x^2 + (B/2)^2}$$

From Eq. 17, it can be deduced that the passive earth pressure acting on unit area dx×dz to be:

$$\sigma_{lateral} = 0.67cK_{pc} + \gamma(-z + (h - 0.5D))K_{p\gamma} \tag{19}$$

Based on the geometry relationship in Fig. 3, forces R_{SBL} and R_{SBR} are equal and can be computed as:

$$R_{SB1} = R_{SBR} = \int_0^{0.5D\sin\theta_f} dx \int_{-\sqrt{(0.5D)^2 - x^2}}^{-(0.5D-h)} \sigma_{lateral} dz \tag{20}$$

Therefore, the bulldozing resistance moments M_{SB} generated by force R_{SBL} and R_{SBR} can be described as:

$$M_{SB} = 2\int_0^{0.5D\sin\theta_f} x dx \int_{-\sqrt{(0.5D)^2 - x^2}}^{-(0.5D-h)} \sigma_{lateral} dz \tag{21}$$

Due to the impacting force and relative motion between wheel side and sand, the unit friction force acting on the area dx×dz can be expressed as following equations by employing the J. Janosi shear theory:

$$\tau_f = (c + \sigma_{lateral}\tan\phi)\left(1 - e^{(-j_{lateral}/K)}\right) \tag{22}$$

where, $j_{lateral}$ is the shear displacement of area dx×dz as the wheel yaws angle β which can be written as:

$$j_{lateral} = \rho\tan\beta = \sqrt{x^2 + (B/2)^2}\tan\beta \tag{23}$$

Then, the resistance moment M_{SF} produced by force R_{SFL} and R_{SFR} can be computed as:

$$M_{SF} = B\int_0^{R\sin\theta_f} dx \int_{-\sqrt{R^2 - x^2}}^{-(R-h)} \tau_f dz \tag{24}$$

Therefore, the resistance moment $M_{lateral}$ acting on the wheel side of wheel can be expressed as:

$$M_{lateral} = M_{SB} + M_{SF} \tag{25}$$

Resultant steering resistance moment: Based on the above analysis, the resultant SRM, M, can be described by the equation:

$$M = M_\tau + M_{long} + M_{lateral} \tag{26}$$

Using the Eq. 26, the SRM can be evaluated, whose value can be used to predict the steering ability and guide the selection of steering motor.

Theoretical effect of D and B on SRM: Figure 4 shows the dependence of SRM on D and B when W = 49N, i = 0.3, $\beta = 25°$.

It can be seen from the Fig. 4 that SRM slightly decrease with the increasing of D when the B is a certain value. The increasing wheel diameter will induce the reducing of wheel sinkage and the contact area between wheel and sand will increase as well as so that the unit radial stress descends at the same time. Therefore, it is difficult to intuitively judge the changing trend of SRM affected by the wheel diameter. According to the calculation from Eq. 16, 18 and 25, the longitudinal and lateral resistance moment descend slightly after raising the value of wheel diameter and holding the value of wheel width. In contrast, the improvement range of shear

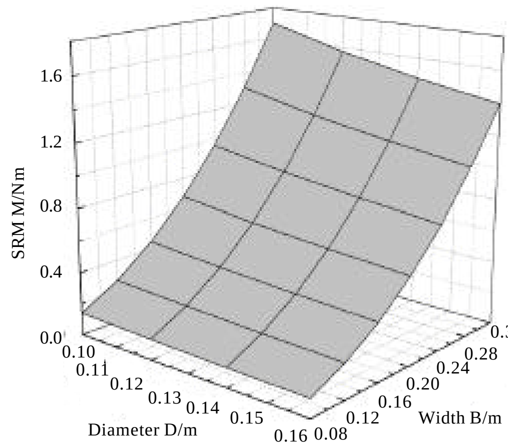

Fig. 4: Dependence of SRM on wheel width and diameter

resistance moment is much less so that the resultant steering resistance moment, M, basically remain the same despite the increasing of wheel diameter.

On the contrary, SRM are significantly improved with the increase of wheel width when the wheel diameter is constant as shown in Fig. 3. The increasing wheel width will reduce the wheel sinkage. However, the theoretical calculation reveals that the longitudinal bulldozing resistance increases sharply to the larger wheel width, meanwhile, the contact area between wheel and sand rise as well as despite of the reduced wheel sinkage. Therefore, the shear resistance moment are raised with the increasing wheel width.

On the basis of the theoretical investigation on wheel steering ability, it can be deduced that the favorable way to improve the steering maneuverability will be to decrease the wheel width. However, the effect of wheel width on wheel traction ability and steering performance is different. Therefore, defining the wheel parameters in designing wheel stage should to balance the motion performance of lunar rover wheel in order to obtaining the optimized wheel configuration parameters.

MOTION PERFORMANCE EVALUATION OF LUNAR ROVER WHEEL

Dimensionless analysis approach: The above analysis reveal that enhancing the wheel motion ability need the opposite changing trend of wheel parameters. A dimensionless analysis is carried out to study the effect of individual wheel parameters on the traction performance and steering ability of lunar rover wheel. Table 2 shows the dimensionless evaluation indexes of motion performance.

Table 2: Dimensionless evaluation indexes of motion performance

Motion performance	Evaluation criterion	Evaluation indexes
Traction performance	Optimum output under the reasonable tractive efficiency	Traction performance index $\Psi = \frac{(P_D / W)^2}{2T_r / (DW)}(1-i)^2$
Steering ability	Flexible steering performance	Steering performance index $\eta_s = \frac{D}{M/W}$

In Table 2, the larger value of η_s illuminates that steering maneuverability is more excellent. The traction performance index, Ψ, is the product of tractive efficiency and drawbar pull under unit weight. The larger value of Ψ indicates that the larger work output under the efficiently tractive efficiency can be generated by the driven wheel.

High tractive efficiency is an object pursued in driving the lunar rover. However, the tractive efficiency does not incorporate the work output of a driven wheel. The possibility exists that in some conditions a device may have high efficiency yet do little work, whereas in other conditions it may do considerable work but have poor efficiency (Pandey and Ojha, 1978). Thus, the work output and tractive efficiency are both required to be combined into one dimensionless term, defined traction performance index, Ψ, as shown in Table 2.

To unmanned lunar rover, it should synchronously possess the excellent traction ability and steering capacity. Therefore, the comprehensive dimensionless evaluation criterion is defined as following:

$$\chi = A_1\psi + A_2\eta_s = A_1\frac{(P_D / W)^2}{2T_r / (DW)}(1-i)^2 + A_2\frac{D}{M / W} \tag{27}$$

where, A_1 and A_2 are the weight coefficient of Ψ and η_s, respectively, whose value can be obtained by means of fuzzy evaluation theory or expert evaluation method.

RESULTS AND DISCUSSION

Here, the evaluation criterions are employed to investigate the reasonable match between wheel diameter and width. In the calculation of evaluation index, the load W is 32.7 N and the sand parameters are assigned as listed in Table 2.

The concept, named width-diameter ratio ζ, is introduced into the motion performance evaluation of lunar rover wheel, whose definition is the ratio of wheel width to wheel diameter. The width-diameter ration is regard as the design index of wheel so as to reflect the reasonable match between wheel width and diameter.

Five samples are selected by combining the different wheel parameters, as shown in Table 3.

Table 3: Analysis samples

	Sample				
	I	II	III	IV	V
B (m)	0.12	0.15	0.15	0.15	0.18
D (m)	0.30	0.33	0.30	0.27	0.30
ζ (m)	0.40	0.45	0.50	0.55	0.6

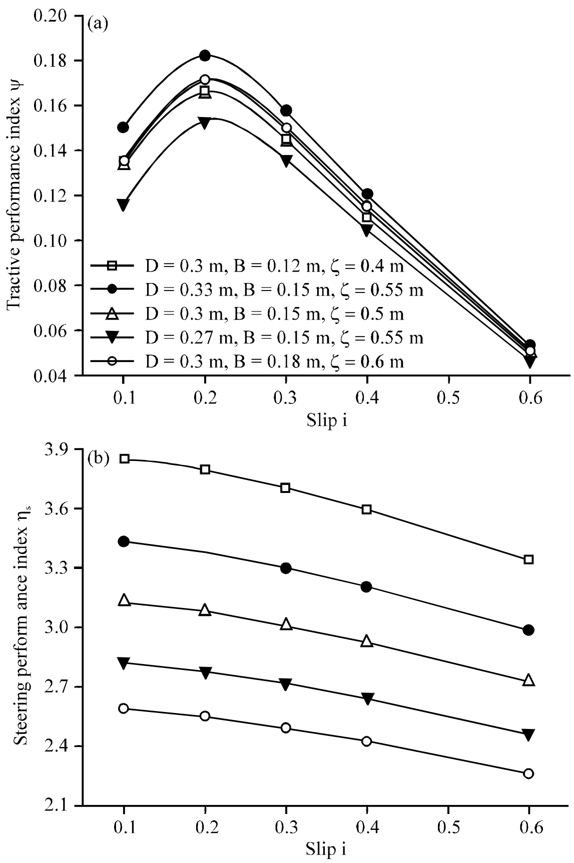

Fig. 5: Dependence of evaluation indexes on slip, respectively

Substituting the parameters of samples (listed in Table 3) in to the Eq. 9, 10, 26 and the evaluation indexes (listed in Table 2), it can derive the dependence of evaluation indexes value on wheel slip as shown in Fig. 5.

To the single evaluation index, it can be observed from the Fig. 5 that the sample exhibits different superiority. However, the results can guide the wheel design in order to enhance a certain item of lunar rover under the specific tasks or a certain terrain conditions.

The manned lunar rover is expected to accomplish many challenging tasks by traveling long distance. When the unknown terrain is so severe that designer can not determine which motion performance item should be enhanced, the comprehensive motion performance of lunar rover should be the research focus so as to ensure

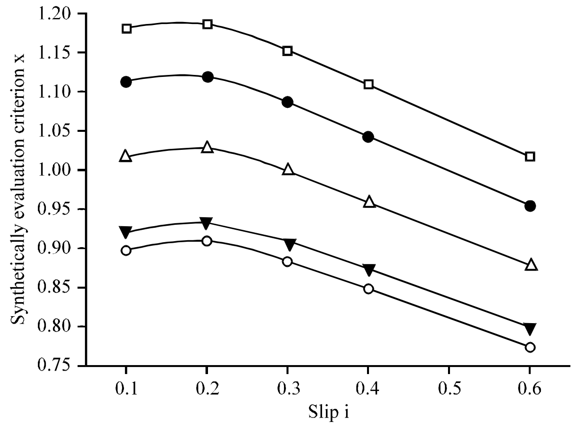

Fig. 6: Dependence of comprehensive evaluation of motion performance for samples at various slip. (—□—) D = 0.3 m, B = 0.12 m, ζ = 0.4; (—●—) D = 0.33 m, B = 0.15 m, ζ = 0.45; (—Δ—) D = 0.3 m, B = 0.15 m, ζ = 0.5; (—▼—) D = 0.27 m, B = 0.15 m, ζ = 0.55; (—○—) D = 0.3 m, B = 0.18, ζ = 0.6

the lunar rover can cope with the tough terrain. Therefore, Eq. 27 is adopted to systematically evaluate the traction ability and steering capacity, where A_1 and A_2 are 0.7 and 0.3, respectively derived by the fuzzy evaluation theory. The Fig. 6 illustrates the dependence of comprehensive evaluation of driving performance for wheel samples at various slip.

The Fig. 6 indicates that the value of χ decreases with the increasing width-diameter ratio, ζ. The maximum value of χ appears at about 20% slip. Therefore, the lower ζ value is advisable when design the wheel in order to improve its comprehensive motion performance.

CONCLUSION

Based on the wheel-sand interaction theory, traction force, driving torque, shear force beneath the steering wheel, bulldozing resistance acting on steering wheel rim and side surface, respectively are investigated. The quantitative relation between these items and wheel parameters is established. And then the theoretical analysis on the effect of wheel parameters on traction performance and steering ability indicates that increasing the wheel diameter is more effective than increasing wheel width in improving the wheel drawbar pull, whereas it is at the cost of increasing the power consumption. In contrast, steering ability is sensitive to rim width. Through the dimensionless evaluation analysis established to study the effect of wheel parameters on the traction performance and steering maneuverability, the results reveal that the samples with different width-diameter ratio exhibit various superiority in single evaluation index which can be utilized to guide the wheel design in order to enhance a certain item of lunar rover under the specific tasks or certain terrain conditions. However, the value of comprehensive evaluation index decreases with the increasing width-diameter ratio, and its maximum value appear at about 20% slip. Therefore, the research results are beneficial to design the wheel in order to enhance lunar rover's comprehensive motion performance on unknown tough terrain.

ACKNOWLEDGMENT

This research was supported by National Natural Science Foundation of China (Grant No. 61005073), Creative Research Fund of Shanghai University, Creative Research Fund for Graduate Student of Shanghai University and the Special Fund of Shanghai University Scientific Selection and Cultivation for Outstanding Young Teachers.

REFERENCES

Bekker, M.G., 1969. Introduction to Terrain-Vehicle Systems. Vol. 1, University of Michigan Press, Ann Arbor, ISBN: 978-0472041442, Pages: 846.

Bigdeli, N., K. Afshar, B.I. Lame and A. Zohrabi, 2008. Modeling of a five-link biped robot dynamics using neural networks. J. Applied Sci., 8: 3612-3620.

Ding, L., H.B. Gao, Z.Q. Deng, K. Nagatani and K. Yoshida, 2011. Experimental study and analysis on driving wheels's performance for planetary exploration rovers moving in deformable soil. J. Terramech., 48: 27-45.

Fang, X., X. Gao, Z. Yin and Q. Zhao, 2011. An efficient process mining method based on discrete particle swarm optimization. Inform. Technol. J., 10: 1240-1245.

Gee-Clough, D. and M.S. Sommer, 1981. Steering forces on undriven, angled wheels. J. Terramech., 18: 25-49.

Hegazy, R.A. and I.S. Dhaliwal, 2011. Evaluation of a power driven residue manager for no-till drills. Asian J. Agric. Res., 5: 127-136.

Irani, R.A., R.J. Bauer and A. Warkentin, 2011. A dynamic terramechanic model for small lightweight vehicles with rigid wheels and grousers operating in sandy soil. J. Terramech., 48: 307-318.

Ishigami, G., A. Miwa, K. Nagatani and K. Yoshida, 2007. Terramechanics-based model for steering maneuver of planetary exploration rovers on loose soil. J. Field Robotics, 24: 233-250.

Kuppan Chetty, R.M., M. Singaperumal and T. Nagarajan, 2011. Distributed formation planning and navigation framework for wheeled mobile robots. J. Applied Sci., 11: 1501-1509.

Liu, J., H. Gao and Z. Deng, 2008. Effect of straight grousers parameters on motion performance of small rigid wheel on loose sand. Inform. Technol. J., 7: 1125-1132.

Liu, J.C., S.L. Tang, Z.Q. Deng, H. Gao, S. Liu and X. Zhou, 2010. Influence analysis of rim radius on motion performance of lunar rover wheel. Proccedings of the International Conference on Mechatronics and Automation (ICMA), August 4-7, 2010, Xian, China, pp: 270-275.

Liu, J.C., H.B. Gao and Z.Q. Deng, 2011. Experimental analysis on effect of grouser circumferential angle on motion performance of lunar rover wheel. Harbin Inst. Technol., 18: 131-137.

Nakashima, H., Y. Shioji, T. Kobayashi, S. Aoki, H. Shimizu, J. Miyasaka and K. Ohdoi, 2011. Determining the angle of repose of sand under low-gravity conditions using discrete element method. J. Terramech., 48: 17-26.

Pandey, K.P. and T.P. Ojha, 1978. Effect of design parameters on the performance of rigid traction wheels on saturated soils. J. Terramech., 15: 145-156.

Peng, L., X. Huang and M. Wang, 2009. Robot map building in unknown dynamic environment based on hybrid dezert-smarandache model. Inform. Technol. J., 8: 284-292.

Raheman, H. and R. Singh, 2003. Steering forces on undriven tractor wheel. J. Terramech., 40: 161-178.

Ray, L.R., D.C. Brande and J.H. Lever, 2009. Estimation of net traction for differential-steered wheeled robots. J. Terramech., 46: 75-87.

Seidi, E., H.R. Ghassemzadeh and A. Salimi, 2009. A cheap automatic tractor's driver assistant system. Asian J. Plant Sci., 8: 451-454.

Wong, J.Y., 2001. Theory of Ground Vehicles. 3rd Edn., John Wiley and Sons Inc., New York, USA., ISBN: 978-0-471-35461-1,.

Xia, K.M., 2011. Finite element modeling of tire/terrain interaction: Application to predicting soil compaction and tire mobility. J. Terramech., 48: 113-123.

Yu, X., H. Gao and Z. Deng, 2008. The research on control of lunar rover with rocker bogie based on bus network driving. Inform. Technol. J., 7: 1001-1008.

Zerigui, A., X. Wu and Z.Q. Deng, 2008. Communication of mobile rover based on FPGA, DSP and wireless communication. Inform. Technol. J., 7: 374-377.